

Applications of the Tsallis Statistics in High Energy Collisions

Trambak Bhattacharyya¹, Jean Cleymans¹, Prakhar Garg², Prateek Kumar³, Sylvain Mogliacci¹, Raghunath Sahoo³, Sushanta Tripathy³

¹ UCT-CERN Research Centre and Department of Physics, University of Cape Town, Rondebosch 7701, South Africa

² Department of Physics and Astronomy, Stony Brook University, SUNY, Stony Brook, New York 11794-3800, USA

³ Discipline of Physics, School of Basic Sciences, Indian Institute of Technology Indore, M.P. 452020, India

E-mail: trambak.bhattacharyya@uct.ac.za

Abstract. We analytically investigate the thermodynamic variables of a hot and dense system in the framework of the Tsallis non-extensive classical statistics in the massless and in the massive cases. In addition to that, we study the effect of Tsallis Power Law distribution on the multi-particle production in the high-energy collisions. The effect of the Tsallis q parameter on the experimentally measured nuclear suppression factor has been investigated, and an attempt to describe the transverse momentum distribution of hadrons produced in high-energy collisions has been made.

1. Introduction

The transverse momentum distributions of hadrons at high energies is very often described by the Tsallis distribution [1]. The PHENIX and STAR collaborations [2, 3] at the Relativistic Heavy Ion Collider (RHIC) at BNL, and the ALICE, ATLAS and CMS collaborations [4, 5, 6, 7, 8] at the Large Hadron Collider (LHC) at CERN have made extensive use of the Tsallis distribution. Tsallis distribution has been very successful in explaining the experimental transverse momentum distribution, longitudinal momentum fraction distribution as well as the rapidity distribution of hadrons in e^+e^- as well as $p-p$ collisions [9, 10, 11, 12, 13, 14, 15].

Also, one can make use of the Tsallis distribution to parameterise the initial distribution of the high-energy particles which, due to interaction with the Quark Gluon Plasma (QGP) medium formed when two heavy ions collide with each other [16], lose energy. The modification of their distribution due to the energy loss sheds light on the characteristics of the QGP medium.

The Tsallis distribution is given by:

$$f = \left[1 + (q-1) \frac{E - \mu}{T} \right]^{-\frac{1}{q-1}}. \quad (1)$$

described by q , the Tsallis q parameter, and the Tsallis temperature T . In our work we use a Thermodynamically consistent form of the Tsallis distribution, f^q , described in detail in [17, 18]. The relevant thermodynamic quantities can be written as integrals over the Tsallis distribution.



2. Analytical calculations of the Tsallis Thermodynamic variables

2.1. Thermodynamic Relations

The entropy density, s , particle number density, n , energy density, ϵ , and the pressure, P in Tsallis thermodynamics are given by [18],

$$s = -g \int \frac{d^3p}{(2\pi)^3} \left[f^q \ln_q f - f \right], \quad (2)$$

$$n = g \int \frac{d^3p}{(2\pi)^3} f^q, \quad (3)$$

$$\epsilon = g \int \frac{d^3p}{(2\pi)^3} E f^q, \quad (4)$$

$$P = g \int \frac{d^3p}{(2\pi)^3} \frac{p^2}{3E} f^q. \quad (5)$$

where g is the degeneracy factor.

The function appearing in Eq. (2) is often referred to as q -logarithm, and is defined by [19]

$$\ln_q(x) \equiv \frac{x^{1-q} - 1}{1 - q}$$

The first and second laws of thermodynamics lead to the following two differential relations:

$$d\epsilon = T ds + \mu dn, \quad (6)$$

$$dP = s dT + n d\mu. \quad (7)$$

where, $s = S/V$ and $n = N/V$ are the entropy and particle number densities, respectively (V is the volume).

It is seen that if we use f^q instead of f to define the thermodynamic variables, the above equations satisfy the thermodynamic consistency conditions which require the following relations to be satisfied:

$$T = \left. \frac{\partial \epsilon}{\partial s} \right|_n, \quad (8)$$

$$\mu = \left. \frac{\partial \epsilon}{\partial n} \right|_s, \quad (9)$$

$$n = \left. \frac{\partial P}{\partial \mu} \right|_T, \quad (10)$$

$$s = \left. \frac{\partial P}{\partial T} \right|_\mu. \quad (11)$$

Eq. (8), in particular, shows that the variable T appearing in Eq. (1) can indeed be identified as a thermodynamic temperature. It is straightforward to show that these relations are indeed satisfied [18].

Analytical calculations of the Tsallis Thermodynamic variables can be approached in the following ways:

Method 1. Taylor's expansion method around $q - 1$

Method 2. The massless limit

Method 3. Employing the Mellin-Barnes contour integration technique

Method 1, detailed in [20], results in very stringent conditions on the energy, temperature and q . In this section we will quote the results of the latter two methods, the details of which can be found in [21].

2.2. Tsallis Thermodynamic variables in the massless limit

Let us define a more general integral,

$$\mathcal{I}(\alpha, \beta) \equiv g \int \frac{d^3 \mathbf{p}}{(2\pi)^3} \frac{p^{\beta-2}}{\left[1 + (q-1) \frac{p-\mu}{T}\right]^{\frac{\alpha}{(q-1)}}}, \quad (12)$$

where, α and β are nothing but handy variables. The former is set either to q or 1 at the end, in order to recover the thermodynamic variables. The above integral is built to converge, in three dimensions, upon some constraints on the various parameters. Those encompass the fact that the integrand shall only assume real values, and the usual infrared and ultraviolet convergence conditions apply. The conditions for the massless case turn out to be

$$1 + \text{Re}(\beta) > 0 \quad , \quad \text{Re}(\alpha) > 0 \quad , \quad (13)$$

$$T > (q-1)\mu \quad , \quad (q-1) < \frac{\text{Re}(\alpha)}{1 + \text{Re}(\beta)}, \quad (14)$$

for which we see that the first two are trivially satisfied, given the actual relevant set of integrals we wish to compute. The last two, on the other hand, are not trivial at all. Given the usual α and β values we are interested in, *e.g.*, some combinations of $\alpha = q, 1$ and $\beta = 2, 3$, we see that q must indeed be bounded at least by $q < 4/3$. This being said, the remaining constraint on the T and μ parameters is either not needed in the case $E_p \geq \mu$, or fulfilled if $m < \mu$ with $q-1 < T/(\mu - E_p)$ and $E_p < \mu$, only here for $m = 0$ in both cases. Notice that this last constraint brings an overall limit for the chemical potential, which is $\mu < 3T$. Thus, we see that this framework must be kept away from asymptotically dense systems. Having said so, we quote the results for different Tsallis Thermodynamic variables in the massless limit.

2.2.1. Number density In the massless limit, the number density can then be obtained from Eq. (12) by setting $\alpha = q$ and $\beta = 2$. Number density in the massless limit can, thus, be written as:

$$n = \frac{g T^3}{2\pi^2} \frac{\left(1 - (q-1) \frac{\mu}{T}\right)^{\frac{2q-3}{q-1}}}{(2-q) \left(\frac{3}{2} - q\right)}. \quad (15)$$

From the above expression, we see that the number density is divergent at $q = 3/2$, 2 which in the light of the previous discussion, implies that the condition of convergence for the corresponding integral is $0 \leq q < 3/2$.

2.2.2. Energy density Similarly, the massless energy density can be obtained from Eq. (12) by setting $\alpha = q$ and $\beta = 3$. Using the same tricks as above, we then arrive at

$$\epsilon = \frac{g T^4}{2\pi^2} \frac{(1 - (q-1)\frac{\mu}{T})^{\frac{3q-4}{q-1}}}{(2-q)(\frac{3}{2}-q)(\frac{4}{3}-q)}. \quad (16)$$

This time, from the above expression, we see that the energy density diverges at $q = 4/3, 3/2, 2$, which again shows that the condition of convergence for the corresponding integral is $0 \leq q < 4/3$, precisely the physically relevant range that we just mentioned.

2.2.3. Pressure In the massless limit, the pressure can be obtained from Eq. (12) by setting $\alpha = q$ and $\beta = 3$, and dividing by 3. Using the same methods as above, this gives us

$$P = \frac{g T^4}{6\pi^2} \frac{(1 - (q-1)\frac{\mu}{T})^{\frac{3q-4}{q-1}}}{(2-q)(\frac{3}{2}-q)(\frac{4}{3}-q)}, \quad (17)$$

and we see that for a system of massless free classical particles following the Tsallis statistics, we indeed have $P = \epsilon/3$. In this case also, divergences arise at $q = 4/3, 3/2, 2$, and the range of convergence is the physically relevant one $1 \leq q < 4/3$.

2.3. Tsallis Thermodynamic variables for systems with massive particles

To compute the Tsallis thermodynamic pressure for a system of massive particles we take the help of the Mellin-Barnes contour integral representation ([22], [23] and [24]) which has been very helpful in Quantum Field Theory in describing the massive propagators in terms of those of the massless ones. Assuming $m \geq \mu$, the Tsallis pressure in the region $(q-1) > T/(m+\mu)$ is given by (for details, see [21]):

$$\begin{aligned} P_U = & \frac{g m^4}{16\pi^{\frac{3}{2}}} \left(\frac{T}{(q-1)m} \right)^{\frac{q}{q-1}} \left[\frac{\Gamma\left(\frac{4-3q}{2(q-1)}\right)}{\Gamma\left(\frac{2q-1}{2(q-1)}\right)} \times {}_2F_1\left(\frac{q}{2(q-1)}, \frac{4-3q}{2(q-1)}, \frac{1}{2}; \left(\frac{(q-1)\mu - T}{(q-1)m}\right)^2\right) \right. \\ & \left. + 2 \left(\frac{(q-1)\mu - T}{(q-1)m} \right) \times \frac{\Gamma\left(\frac{3-2q}{2(q-1)}\right)}{\Gamma\left(\frac{q}{2(q-1)}\right)} \times {}_2F_1\left(\frac{2q-1}{2(q-1)}, \frac{3-2q}{2(q-1)}, \frac{3}{2}; \left(\frac{(q-1)\mu - T}{(q-1)m}\right)^2\right) \right] \end{aligned} \quad (18)$$

Pressure in the region $(q-1) < T/(m+\mu)$ can be obtained (see [21]) by analytically continuing the hypergeometric functions using [25]. Other thermodynamic variables for the system of massive particles can be obtained using the Thermodynamic relations and the chain rules for the partial derivative of the hypergeometric functions.

3. Description of multi-particle production using the Tsallis distribution

In this part of the work, we represent the initial distribution of the energetic particles with the help of the Tsallis power law distribution parameterized by the Tsallis q parameter and the Tsallis temperature T , remembering the fact that their genesis is due to very hard scatterings. We plug the initial distribution (f_{in}) in the Boltzmann Transport Equation (BTE) and solve it with the help of the Relaxation Time Approximation (RTA) of the collision term to find out

the final distribution (f_{fin}). The ratio expressible in terms of q and T can be computed and compared with the experimentally observed values of R_{AA} which is theoretically represented as:

$$R_{AA} = \frac{f_{fin}}{f_{in}} \quad (19)$$

and can be compared with experimentally measured R_{AA} given by:

$$R_{AA}(p_T) = \frac{(1/N_{AA}^{evt})d^2N_{AA}/dydp_T}{(\langle N_{coll} \rangle / \sigma_{NN}^{inel}) \times d^2\sigma_{pp}/dydp_T}, \quad (20)$$

where $d^2N_{AA}/dydp_T$ is the yield in A+A collisions, $\langle N_{coll} \rangle$ is the number of binary nucleon-nucleon collisions averaged over the impact parameter range of the corresponding centrality bin calculated by Glauber Monte-Carlo simulation [26]. σ_{NN}^{inel} is the inelastic cross section and $d^2\sigma_{pp}/dydp_T$ is the differential cross section for inelastic $p + p$ collisions. N_{AA}^{evt} is the number of events in A+A collisions.

The evolution of the particle distribution owing to its interaction with the medium particles can be studied through BTE,

$$\frac{df(\vec{x}, \vec{p}, t)}{dt} = \frac{\partial f}{\partial t} + \vec{v} \cdot \vec{\nabla}_x f + \vec{F} \cdot \vec{\nabla}_p f = C[f], \quad (21)$$

where $f(\vec{x}, \vec{p}, t)$ is the distribution of particles which depends on position, momentum and time. \vec{v} is the velocity and \vec{F} is the external force. $\vec{\nabla}_x$ and $\vec{\nabla}_p$ are the partial derivatives with respect to position and momentum, respectively. $C[f]$ is the collision term which encodes the interaction of the probe particles with the medium. Assuming homogeneity of the system ($\vec{\nabla}_x f = 0$) and absence of external force ($\vec{F} = 0$), the second and third terms of the above equation become zero and Eq. (21) becomes,

$$\frac{df(\vec{x}, \vec{p}, t)}{dt} = \frac{\partial f}{\partial t} = C[f] \quad (22)$$

In the relaxation time approximation [27], the collision term can be expressed as,

$$C[f] = -\frac{f - f_{eq}}{\tau} \quad (23)$$

where f_{eq} is Boltzmann local equilibrium distribution characterized by a temperature T_{eq} . τ is the relaxation time, the time taken by a non-equilibrium system to reach equilibrium. With the ansatz in Eq. (23), Eq. (22) becomes,

$$\frac{\partial f}{\partial t} = -\frac{f - f_{eq}}{\tau} \quad (24)$$

Solving the above equation in view of the initial conditions i.e. at $t = 0, f = f_{in}$ and at $t = t_f, f = f_{fin}$ leads to,

$$f_{fin} = f_{eq} + (f_{in} - f_{eq})e^{-\frac{t_f}{\tau}}, \quad (25)$$

where t_f is the freeze-out time. Using Eq. (25), the nuclear modification factor can be expressed as,

$$R_{AA} = \frac{f_{fin}}{f_{in}} = \frac{f_{eq}}{f_{in}} + \left(1 - \frac{f_{eq}}{f_{in}}\right) e^{-\frac{t_f}{\tau}} \quad (26)$$

Eq.(26) is the derived nuclear modification factor after incorporating relaxation time approximation [27], which is the basis of our analysis. It involves the (power law-like) initial distribution and the equilibrium distribution. In this analysis, the initial distribution is parameterized using the thermodynamically consistent Tsallis distribution [18] at $\mu = 0$.

$$f_{in} = \frac{gV}{(2\pi)^2} p_T m_T \left[1 + (q-1) \frac{m_T}{T} \right]^{-\frac{q}{q-1}}, \quad (27)$$

where $m_T = \sqrt{p_T^2 + m^2}$, for a particle with mass m , g is the degeneracy and V is the volume of the system. The nuclear modification factor can be expressed as,

$$R_{AA} = \frac{e^{-\frac{m_T}{T_{eq}}}}{(1 + (q-1) \frac{m_T}{T})^{-\frac{q}{q-1}}} + \left[1 - \frac{e^{-\frac{m_T}{T_{eq}}}}{(1 + (q-1) \frac{m_T}{T})^{-\frac{q}{q-1}}} \right] e^{-\frac{t_f}{\tau}} \quad (28)$$

This will be used as the fitting function to the experimental results in the next section.

3.1. Results and Discussion

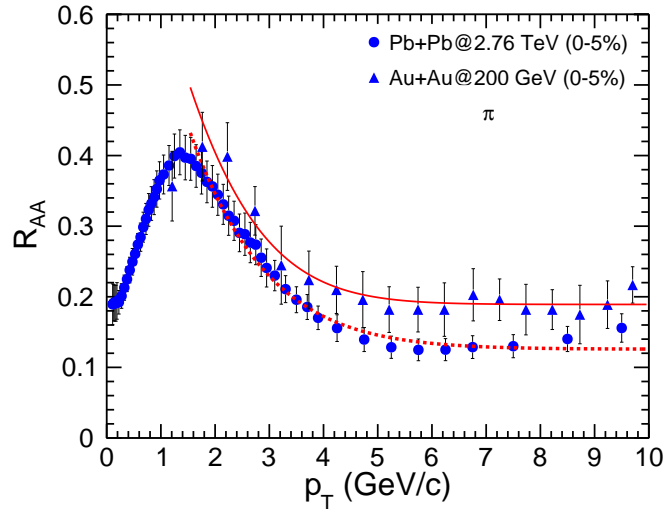


Figure 1. Fitting of experimental data for nuclear modification factor with our proposed model for π^0 [29] (blue triangles) in Au+Au collisions at $\sqrt{s_{NN}} = 200$ GeV, and $\pi^+ + \pi^-$ [30] in Pb+Pb collisions at $\sqrt{s_{NN}} = 2.76$ TeV (blue dots). The solid red line shows the fitting for blue triangles and the dotted red line shows the fitting for blue dots.

We now proceed to the more detailed analysis of the experimental data with the model proposed above. Keeping all the parameters free, we fit the spectra for different particles in different centralities for Pb+Pb and Au+Au collisions using the TMinuit class available in the ROOT library [28] to get a convergent solution. The convergent solution is obtained by χ^2 minimization technique. Here T , q and t_f/τ are the fitting parameters for the experimental data. The equilibrium temperature T_{eq} is fixed to 160 MeV throughout the analysis.

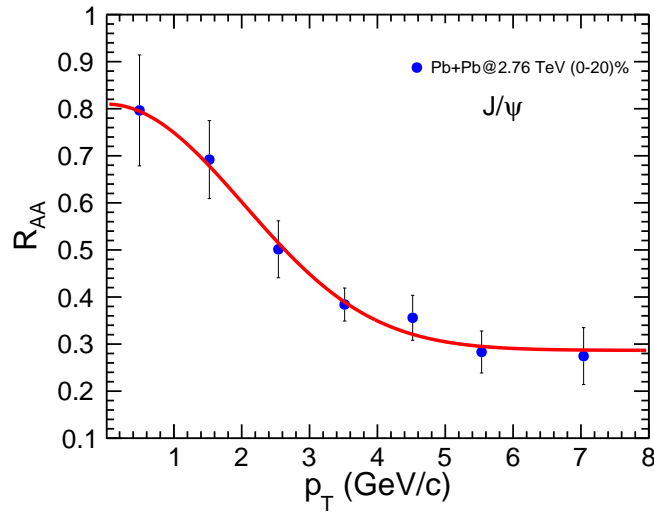


Figure 2. Fitting of experimental data for nuclear modification factor with our proposed model for J/ψ [31] in Pb+Pb collisions at $\sqrt{s_{NN}} = 2.76$ TeV (blue dots) with centrality (0-90)%. The solid red line shows the fitting to the experimental data.

Fig. (1) shows the fitting of experimental data using Eq. (28) for the π^0 meson in the most central Au+Au collisions at $\sqrt{s_{NN}} = 200$ GeV. The derived expression for R_{AA} fits the data in intermediate to high- p_T range. Also, in Fig. (1) we show the fitting of experimental data for $\pi^+ + \pi^-$ in most central Pb+Pb collisions at $\sqrt{s_{NN}} = 2.76$ TeV. The model considered here, fits the data from intermediate to high- p_T range with the parameter values: $q = 1.00151 \pm 0.00149$, $T = 0.17854 \pm 0.00143$, $t_f/\tau = 2.07313 \pm 0.061906$.

In our analysis, it is observed that the fitting of low p_T for light flavour particles fails due to the reason that it involves different physical processes such as regeneration, coalescence, shadowing etc., which are out of the scope of the present formalism. But in heavy flavour particles, no such processes are involved at the discussed energies. Thus, our proposed model explains successfully the heavy flavour R_{AA} data (J/ψ for example) with the fitting parameters $q = 1.01252 \pm 0.00998$, $T = 0.14676 \pm 0.01408$, $t_f/\tau = 1.06248 \pm 0.157049$. Analysis for the other particle species can be found in [16].

4. Summary and Conclusion

In the present paper, we have discussed about the two different applications of the Tsallis distribution in the field of high energy collisions. In the first part, we have discussed about the analytical calculation of the Tsallis Thermodynamic variables in the massless limit, and in the massive limit. In the latter case, we have used the Mellin-Barnes contour integral representation which is used in Quantum Field Theory to represent the massive propagators in terms of the massless ones. The calculations may be particularly important in reducing the cumbersome momentum integrals, so far performed numerically, into simpler analytic expressions.

In the second part of the paper, we have discussed about the application of the Tsallis Statistics in the multi-particle production and their nuclear modification factor. We have seen that the J/ψ data is well explained once we parameterize the initial distributions using the Tsallis distribution. The same inference can be drawn for the other heavy flavours as well.

Acknowledgements

T. B. acknowledges the University of Cape Town Research Committee (South Africa) for support. S. M. would like to acknowledge the financial support from the Claude Leon Foundation (South Africa).

References

- [1] Tsallis C 1988 *J. Statist. Phys.* **52** 479
- [2] Abelev B I *et al.* (STAR collaboration) 2007 *Phys. Rev. C* **75** 064901
- [3] Adare A *et al.* (PHENIX collaboration) 2011 *Phys. Rev. D* **83** 052004
- [4] Aamodt K *et al.* (ALICE collaboration) 2010 *Phys. Lett. B* **693** 53
- [5] Aamodt K *et al.* (ALICE collaboration) 2011 *Eur. Phys. J C* **71** 1655
- [6] Abelev B *et al.* (ALICE collaboration) 2012, *Phys. Rev. Letts.* **109** 252301
- [7] Khachatryan V *et al.* (CMS collaboration) 2010 *J. of High Eng. Phys.* **02** 041
- [8] Aad G *et al.* (ATLAS collaboration) 2011 *New J. Phys.* **13** 053033
- [9] Bediaga I, Curado E M F and Miranda J M de 2000 *Physica A* **286** 156.
- [10] Wilk G and Włodarczyk Z 2015 *Acta Phys. Polon. B* **46** 1103
- [11] Ürmösy K, Barnaföldi G G and Biró T S 2011 *Phys. Lett. B* **701** 111
- [12] Ürmösy K, Barnaföldi G G, and Biró T S 2012 *Phys. Lett. B* **718** 125.
- [13] Khandai P K, Sett P, Shukla P and Singh V 2013 *Int. Jour. Mod. Phys. A* **28** 1350066
- [14] Li B -C, Wang Y -Z and Liu F -H 2013 *Phys. Lett. B* **725** 352
- [15] Marques L, Cleymans J and Deppman A 2015 *Phys. Rev. D* **91** 054025
- [16] Tripathy S, Bhattacharyya T, Garg P, Kumar P, Sahoo R, and Cleymans J 2016 *Eur. Phys. J A* **52** 289
- [17] Cleymans J and Worku D 2012 *J. Phys. G* **39** 025006
- [18] Cleymans J and Worku D 2012 *Eur. Phys. Jour. A* **48** 160
- [19] Tsallis C 2009 *Introduction to Nonextensive Statistical Mechanics* (New York: Springer Science+Business Media)
- [20] Bhattacharyya T, Cleymans J, Khuntia A, Pareek P and Sahoo R 2016 *Eur. Phys. J A* **52** 30
- [21] Bhattacharyya T, Cleymans J and Mogliacci S 2016 *Phys. Rev. D* **94** 094026
- [22] Smirnov V A 2004 *Evaluating Feynman Integrals* (Berlin: Springer-Verlag) .
- [23] Boos E E and Davydychev A I 1991 *Theor. Math. Phys.* **89** 1052
- [24] Davydychev A I and Tausk J B 1993 *Nucl. Phys. B* **397** 123
- [25] Bateman H 1953 *Higher Transcendental Functions* (New York: McGraw-Hill Book Company) (See Section 2.10 formula (4), and the conditions therein)
- [26] Glauber R J and Matthiae G 1970 *Nucl. Phys. B* **21** 135.
- [27] Balescu R 1975 *Equilibrium and Non-Equilibrium Statistical Mechanics* (USA: John Wiley and Sons).
- [28] CERN ROOT V.5.34/32 (June 23, 2015) Package: <http://root.cern.ch>.
- [29] Adare A *et al.* (PHENIX Collaboration) 2008 *Phys. Rev. Lett.* **101** 232301
- [30] Abelev B B *et al.* (ALICE Collaboration) 2014 *Phys. Lett. B* **736** 196
- [31] Abelev B B *et al.* (ALICE Collaboration) 2014 *Phys. Lett. B* **734** 314